Part 1- Geometric Calibration of Pinon Corner Reflectors
Part 2 - Interferometric Processing and Calibration

David Sandwell, Yuri Fialko, and Meng Wei
October 10, 2006 - CVST#5

JAXA has provided 16 PALSAR images in FBS Mode for our calibration/validation research. The data are selected from three orbital tracks and have look angles of either 34.3˚ or 41.5˚. Figure 1 shows the data frames in relation to the geography of the area.
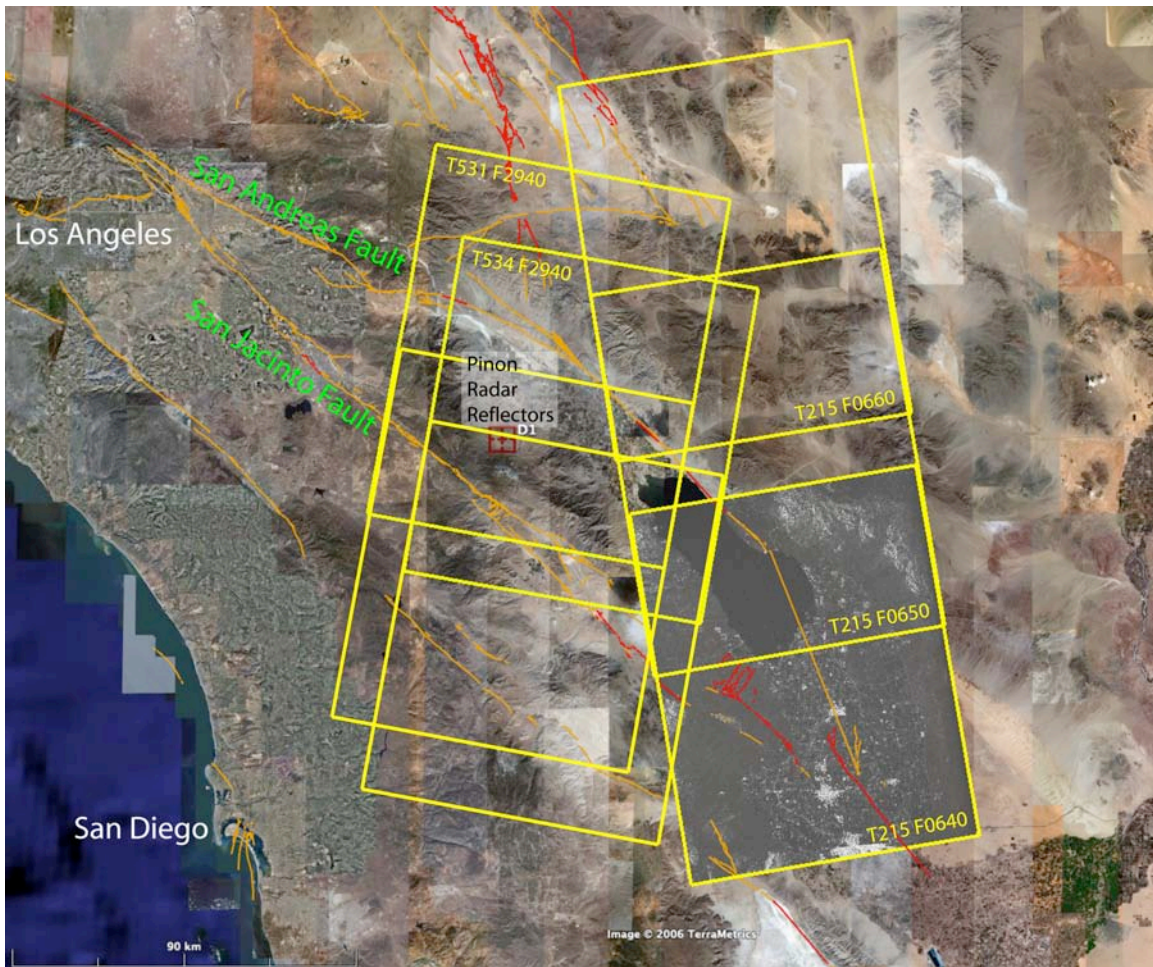

Figure 1. Location map for Pinon corner reflectors. Reflectors lie between the San Andreas and San Jacinto Faults.   PALSAR data (L1.0) are used for both geometric and interferometric calibration. Frame positions are based on radar images.

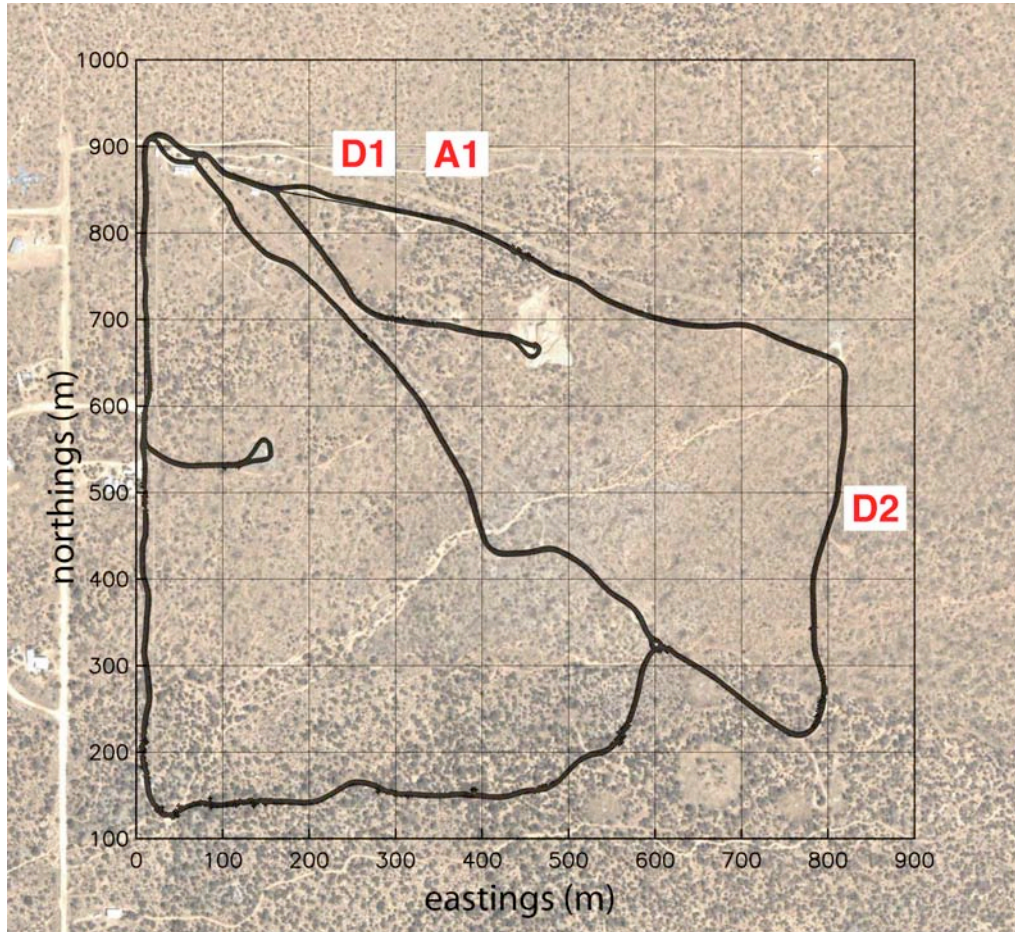# Part 1 - Geometric Calibration of Pinon Corner Reflectors

Figure 2. Satellite image of the Pinon Flat Observatory. This arid region at an elevation of 1200 m is relatively flat with a surface of decomposed granite sparsely covered by bush and grass. Three radar corner reflectors are oriented to reflect energy from ascending (A1) and descending (D1 and D2) passes of ALOS.

GPS-Coordinates of Radar Reflectors

	position			orientation	
	lat	lon	height	elevation	azimuth
A1	33.612246	-116.456768	1258.990	39°	257.5°
D1	33.612253	-116.457893	1257.544	39°	102.5°
D2	33.607373	-116.451836	1254.537	39°	102.5°

Latitude and longitude in decimal degrees and elevation in meters relative to the WGS-84 co-ordinate system and ellipsoid.
The survey point is the apex (lowest corner) of each reflector. There should be a correction for the offset between the phase center of the reflector and the apex.

Comparison of positions in Range/Azimuth Coordinates

JAXA delivered 16 Level 1.0 images. Five of the images illuminate the corner reflectors. We have analyzed the following three images for geometric calibration.

```
product              modepath frame  A/D  date      look  level
ALPSRP019792940      FBS  534  2940   D   6/8/06     34.3  1.0
ALPSRP026502940      FBS  534  2940   D   7/24/06    34.3  1.0
ALPSRP033212940      FBS  534  2940   D   9/8/06     34.3  1.0
```

Positions based on orbit - We used the timing data from the IMG-file and the orbit data from the LED-file to map the positions of the reflectors from lat, lon, height to range, azimuth pixel co-ordinates. Here is the algorithm.
1) Convert the positions from lat, lon, height to x, y, z coordinates using a WGS84 ellipsoid.
2) Compute the x, y, z position of ALOS at the times of all the echoes of the SAR image.
3) Find the echo that has the minimum distance between the reflector and ALOS.
4) Record the range and azimuth of this minimum distance for each reflector.

Positions based on images - We focussed the images in our SAR processor omitting the first 3584 lines since this corresponds to ½ the length of the synthetic aperture. The three images have small Doppler centroids of -3.4 Hz -74 Hz and -61.5 so we processed them with an average value of -35 Hz. We then observed the offsets visually and recorded the pixel position. The accuracy of the range position is +/- 1 pixel while the azimuth accuracy is +/- 2 pixel.

Offset Results

image/ reflector	Ro	Ri	dR	Ao	Ai	dA
ALPSRP019792940 D1	7586	7596	-10	17720	15717	2003
ALPSRP019792940 D2	7497	7507	-10	17858	15855	2003
ALPSRP026502940 D1	7469	7479	-10	17580	15579	2001
ALPSRP026502940 D2	7380	7390	-10	17718	15717	2001
ALPSRP033212940 D1	7906	7916	-10	17779	15777	2002
ALPSRP033212940 D2	7817	7827	-10	17918	15915	2003
average			**-10.0**			**2002.2**

Ro - range position of reflector derived from orbital information
Ri - range position of reflector derived observed in amplitude image
Ao - range position of reflector derived from orbital information
Ai - range position of reflector derived observed in amplitude image

Summary of Results

Range - The average offset in range is -10.0 pixel = -46.9m = -0.31 microseconds. The sign of the offset shows the range in the image longer than the range from the orbit. This could be due to ionospheric path delay. This estimate of -0.31 is close to the -0.36 microsecond recommended by Shimada at CVST#4.

Azimuth - The average offset in azimuth is 2002.2 pixels = 0.929 s (prf=2155Hz). This is close to the 1-second recommended by Shimada.

Part 2 - Interferometric Processing and Calibration

PALSAR interferometry has a few significant differences from C-band interferometry such as ERS or Envisat. This required some changes and improvements to our existing InSAR code.

1. Proper focus of the image requires a more precise estimate of the **Doppler rate parameter**.

2. Because the range resolution of PALSAR is about 2 times better than ERS and Envisat, the alignment of the reference and repeat images in the range direction must be about two times more precise. We have adopted a **6-parameter model** to warp the repeat image onto the reference image. The parameters are: shift (r+a), range stretch (r+a), and azimuth stretch (r+a).

3. In addition the 2 times higher range resolution coupled with the 4 times longer wavelength and larger look angle increase the critical baseline of PALSAR to as large as 18 km. In comparison the critical baseline for ERS is ~1 km. The ability to use much longer baseline pairs causes an **elevation-dependent range shift** that must be corrected.

1. Improved estimation of Doppler rate parameter

Proper focusing of a SAR image requires knowing the range R between the satellite and a reflector on the ground as a function of slow time s. This function is commonly approximated by a parabola.

$$R(s) = R_o + \dot{R}_o(s - s_o) + \frac{\ddot{R}_o}{2}(s - s_o)^2 + \dots$$

The three terms can be estimated by selecting a target reflector on the ground within the the image and calculating the range to the reflector using the precise orbital information stored in the PALSAR LED-file. An example of the range versus time is shown in Figure 3. We use the curvature of the polynomial $\ddot{R}_o$ to estimate the Doppler rate for our SAR processor. $f_r = \frac{2\ddot{R}_o}{\lambda}$
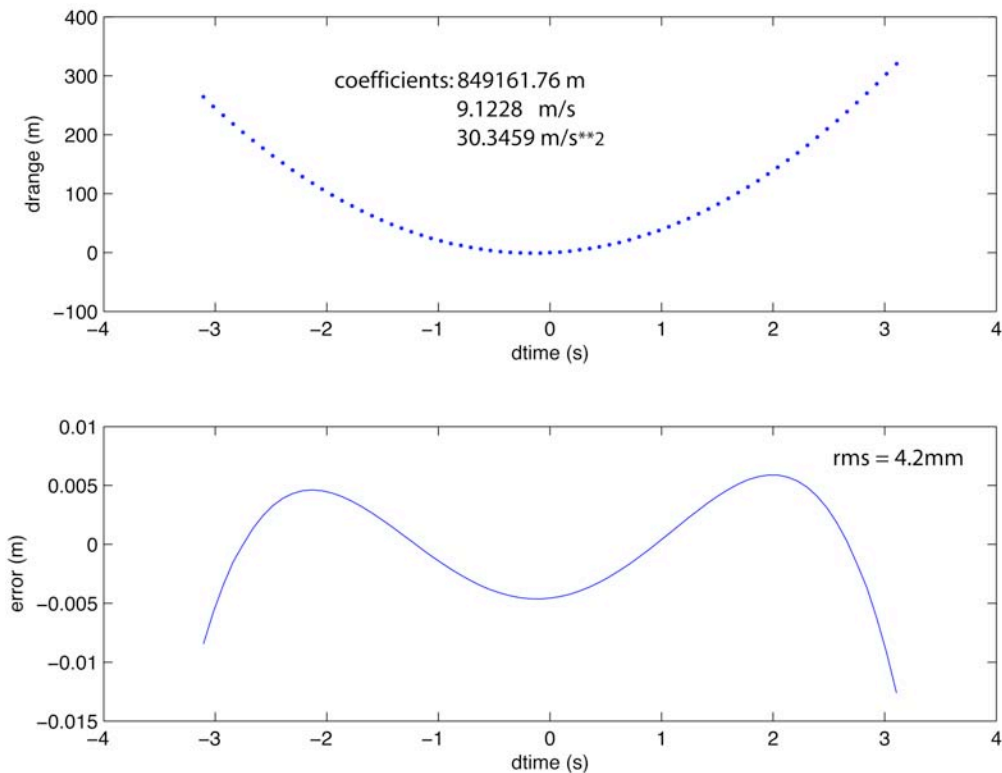

Figure 3. Range versus time between ALOS and a reflector in the near range of the SAR image. The parabolic approximation has a maximum error of about 1 cm at a time offset of 3 seconds. This corresponds to a small fraction of the 23-cm wavelength. Note that the actual aperture length for ALOS is only +/- 1.5 seconds so this approximation is justified.

2. Image alignment with 6-parameter model

Achieving interferometric phase correlation requires image alignment at to an accuracy of better than 1 pixel in both range and azimuth. We were fortunate to have our first interferometric pair with a relatively short baseline of 1060 m. Other pairs we have considered have longer baselines of 2000 to 3000 km so the alignment issues are more challenging. After alignment of the reference and repeat image, we re-computed the image offsets (Figure 4). In general the 6-parameter model reduces the offsets to less than 1 pixel. However we have found the range offsets can exceed 0.6 pixel in areas of high relief.
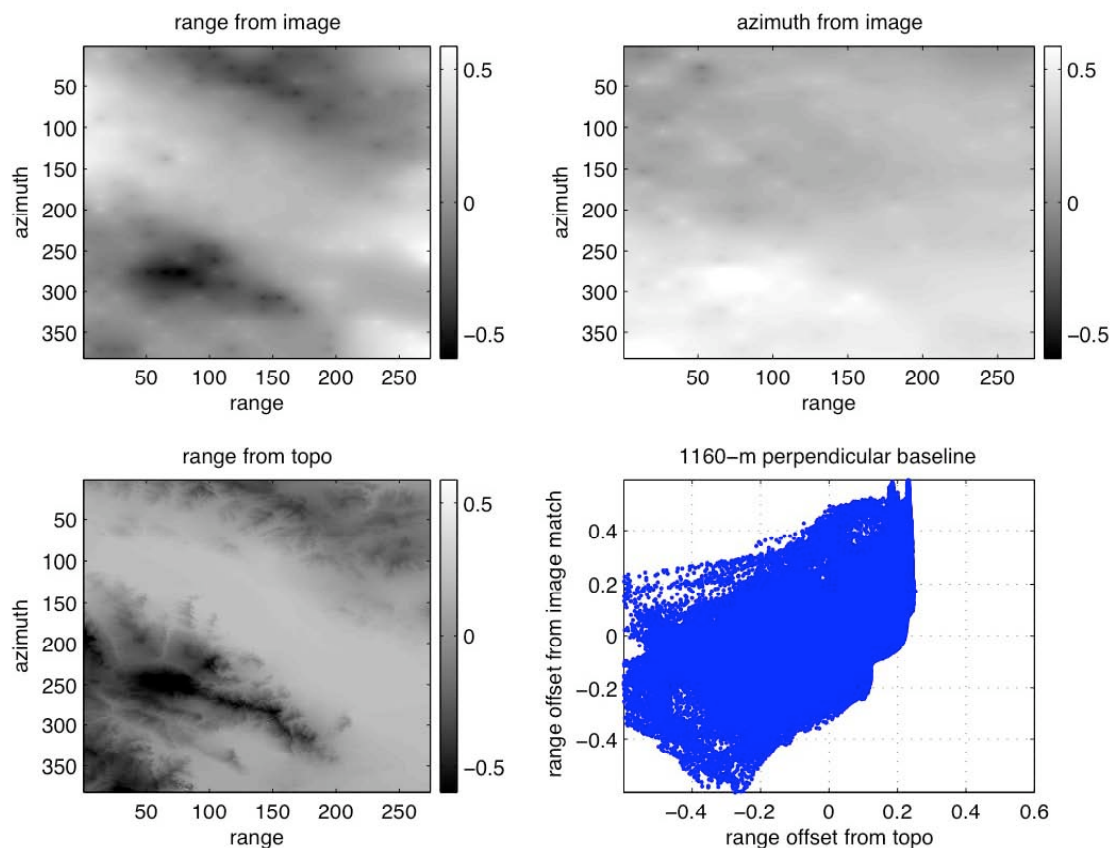
Figure 4. (top) residual range and azimuth offsets after 6-parameter image alignment. (bottom) residual range offset based on stereoscopic effect of 1060-m baseline shows correlation with topography.

3. Correcting the elevation-dependent range shift

We implemented an elevation-dependent range correction based on the orbital geometry by interpolating the range lines of the repeat image just prior to forming the interferogram. This requires mapping the topography into the range/azimuth coordinate system of the single-look complex SAR images. This is done using precise orbital information and a single control point in the image. The correlation maps (Figure 5) show the improvement in areas of high relief due to this correction.
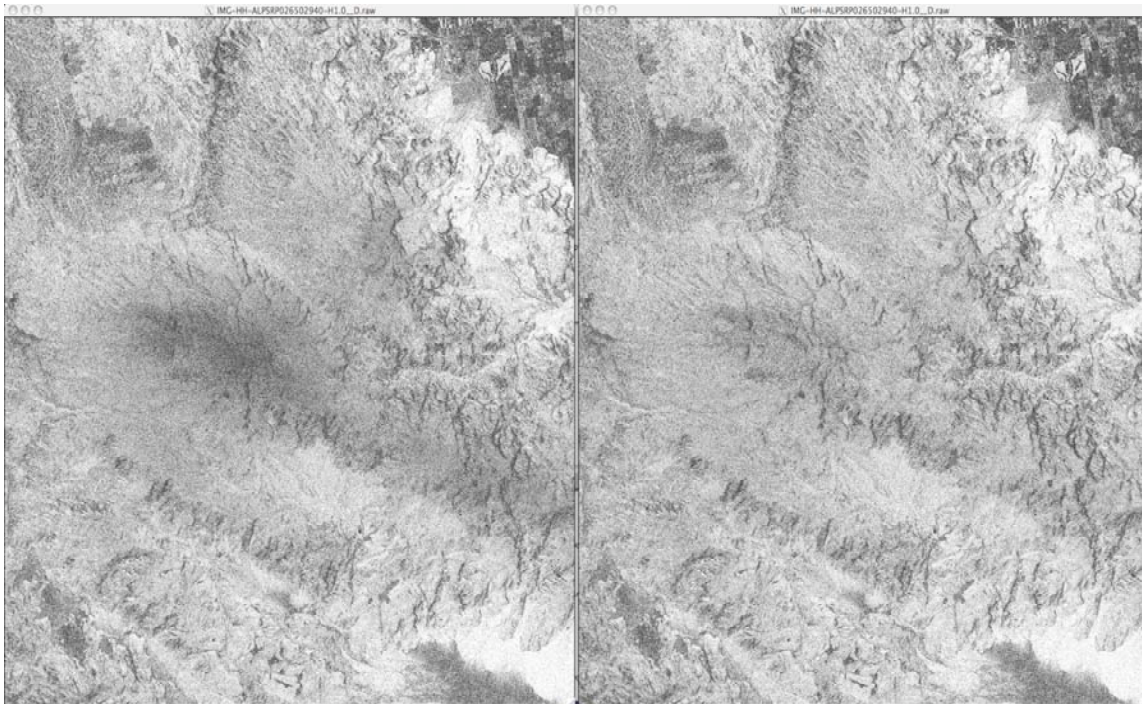
Figure 5. Correlation maps where white has correlation greater than 0.8 and black is zero correlation. (left) correlation without elevation-dependent correction shows low correlation at the highest elevation. (right) correlation using elevation-dependent correction shows improvement in areas of extreme relied, both high and low.

Final interferogram

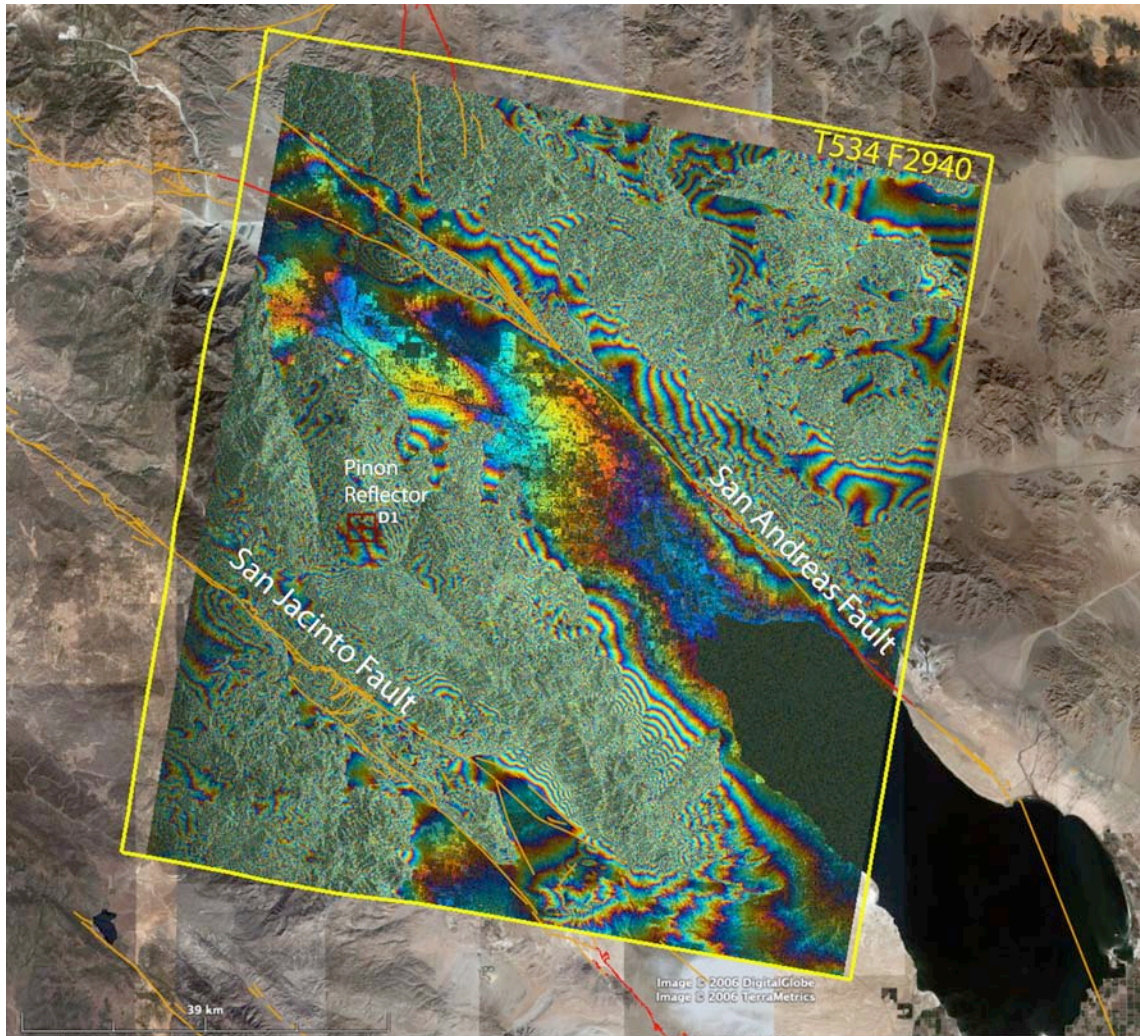Results from our first interferometric analysis follow.

Figure 6. Interferometric phase with respect to a spherical earth reveals a high fringe rate due to topography. Correlation for this 46-day, 1060-m baseline interferogram is **excellent**. Spatial resolution is 2 times better than ERS and Envisat resulting in more precise interferometric fringes.
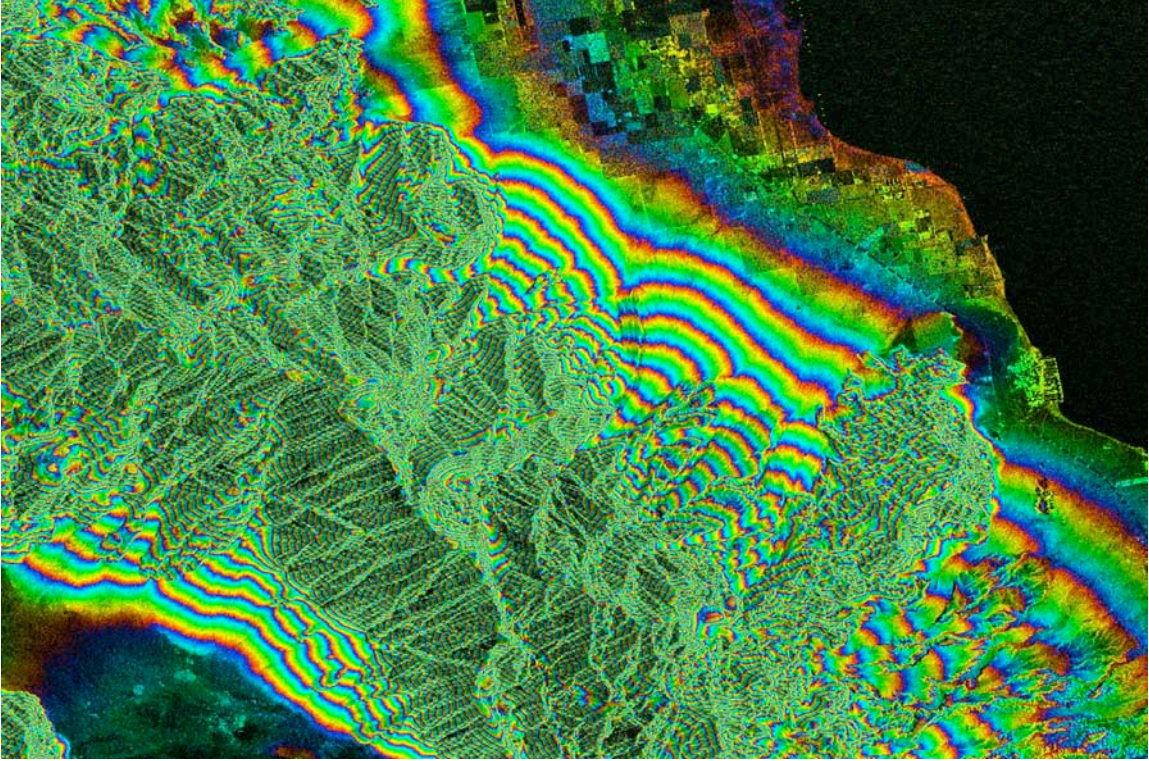
Figure 6. Blow-up of interferogram shown in Figure 5 reveals the excellent coherence and high fringe rate due to topography.
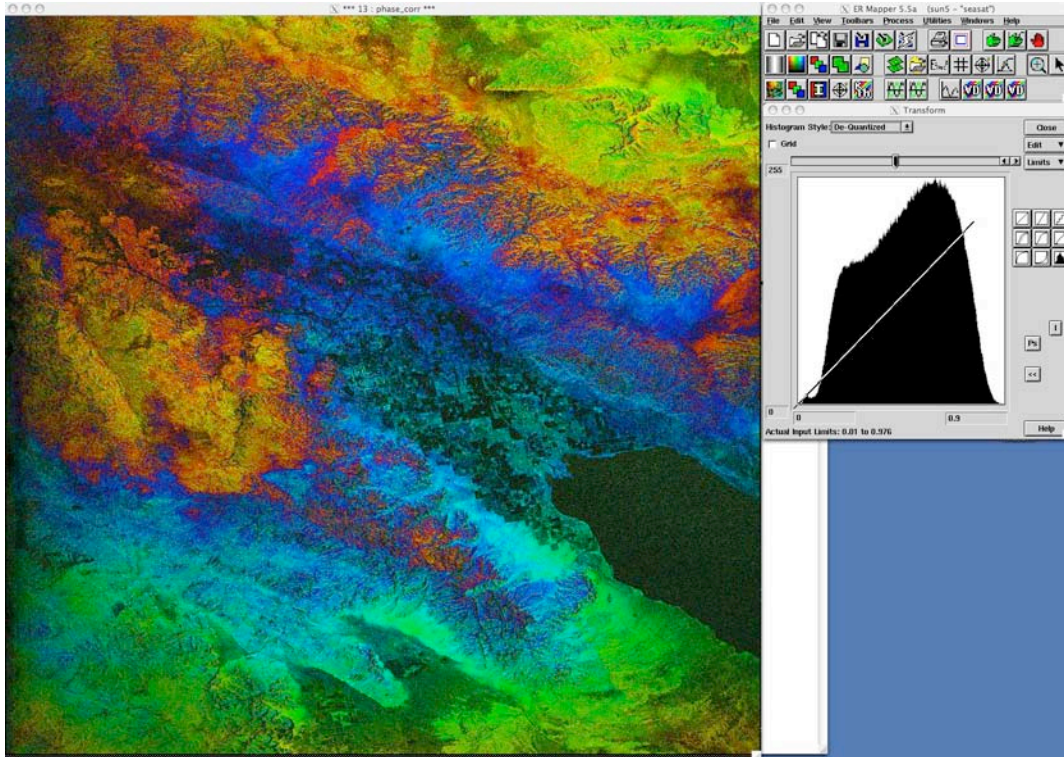
Figure 7. Interferogram with topographic fringes removed. There is a 1-fringe (12-cm) N/S trend that is not accounted for in the processing. This is either due to errors in the processing software, orbital error, or ionospheric delay. Understanding this long-wavelength trend will require processing of many more PALSAR interferograms. The plot on the right shows the histogram of interferometric correlation between 0 and 0.8.

We have processed two other interferograms having perpendicular baselines of 1225 m and 2242 m. Phase recovery is excellent even for the longer baseline, although there are 10 residual fringes (1.2 m) across the image (Figure 8). These could be due to orbit error or ionospheric delay. Investigating the origin of the residual fringes should be a high priority research topic. In addition to the phase ramp across the image, there is residual phase at a smaller scale (Figure 9). This is due to errors in the SRTM topography model.
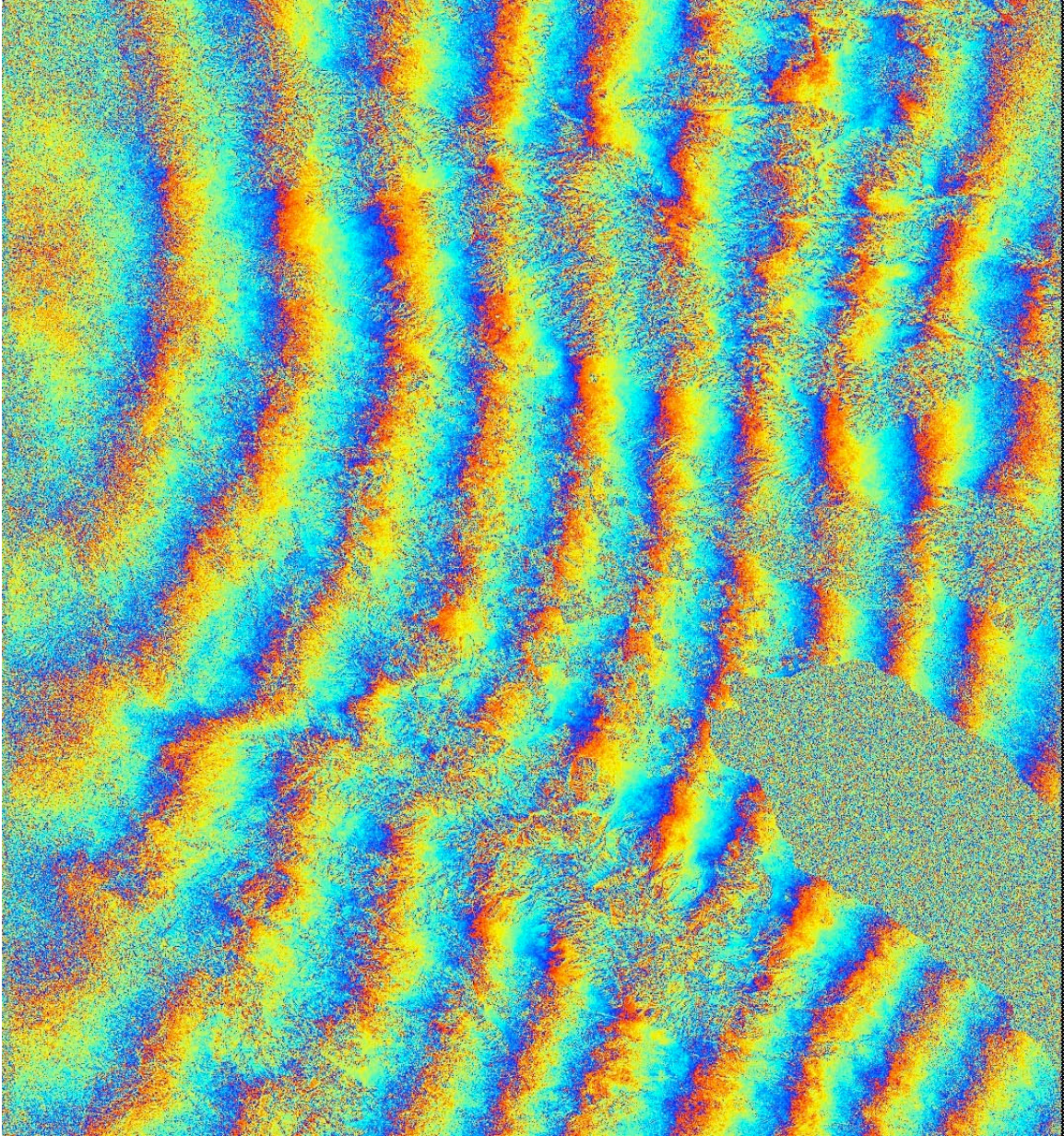
Figure 8. ALOS interferogram with 135-day temporal baseline and 2236 perpendicular
baseline. The 10 residual fringes across the image are either due to orbit error or
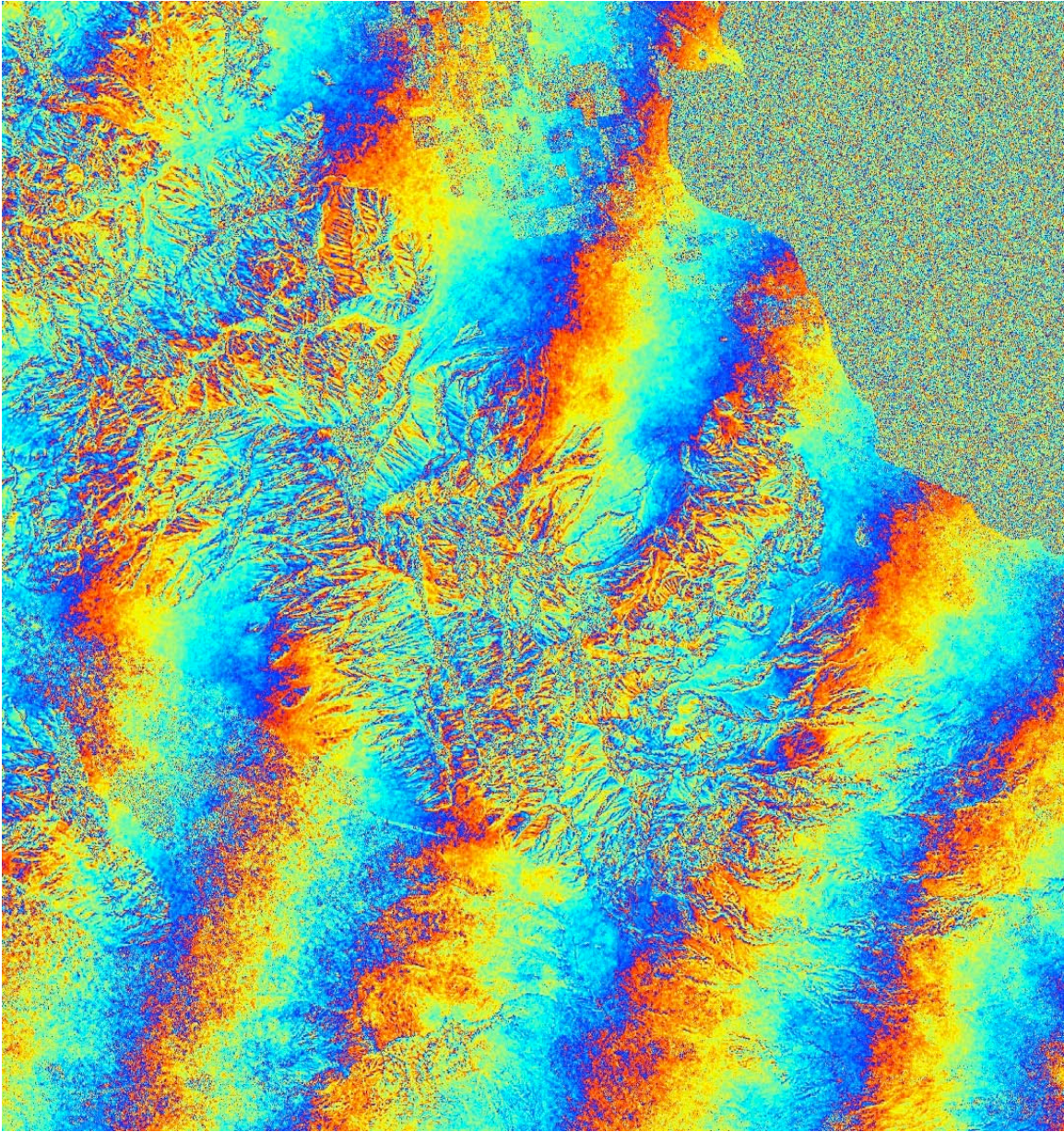ionospheric delay.

Figure 9. Zoom of same interferogram in Figure 8 having a 135-day temporal baseline and 2236 m perpendicular baseline. Salton Sea provides scale. The small-scale residual fringes in the mountain areas are due to errors in the SRTM topography model.